

Quantum criticality and spin liquid phase in the Shastry-Sutherland model

Jianwei Yang,¹ Anders W. Sandvik^{1,2,3,*} and Ling Wang^{1,4,†}

¹Beijing Computational Science Research Center, 10 East Xibeiwang Road, Beijing 100193, China

²Department of Physics, Boston University, 590 Commonwealth Avenue, Boston, Massachusetts 02215, USA

³Beijing National Laboratory for Condensed Matter Physics and Institute of Physics, Chinese Academy of Sciences, Beijing 100190, China

⁴Department of Physics, Zhejiang University, Hangzhou 310000, China



(Received 25 April 2021; accepted 8 February 2022; published 23 February 2022)

Using the density-matrix renormalization group method for the ground state and excitations of the Shastry-Sutherland spin model, we demonstrate the existence of a narrow quantum spin liquid phase between the previously known plaquette-singlet and antiferromagnetic states. Our conclusions are based on the finite-size scaling of excited level crossings and order parameters. Together with previous results on candidate models for deconfined quantum criticality and spin liquid phases, our results point to a unified quantum phase diagram where the deconfined quantum-critical point separates a line of first-order transitions and a gapless spin liquid phase. The frustrated Shastry-Sutherland model is close to the critical point but slightly inside the spin liquid phase, while previously studied unfrustrated models cross the first-order line. We also argue that recent heat capacity measurements in $\text{SrCu}_2(\text{BO}_3)_2$ show evidence of the proposed spin liquid at pressures between 2.6 and 3 GPa.

DOI: [10.1103/PhysRevB.105.L060409](https://doi.org/10.1103/PhysRevB.105.L060409)

The quasi-two-dimensional (2D) $S = 1/2$ quantum magnet $\text{SrCu}_2(\text{BO}_3)_2$ [1–3] has emerged [4–9] as the most promising realization of a deconfined quantum-critical point (DQCP) [10–12], where a state spontaneously forming a singlet pattern meets an antiferromagnetic (AFM) state in a phase transition associated with fractionalized excitations (spinons). The intralayer interactions of the Cu spins correspond to the Shastry-Sutherland (SS) model [13], with highly frustrated AFM interdimer (J) and intradimer (J') Heisenberg couplings. The SS model has three known ground states versus $g = J/J'$: a dimer singlet (DS) state for small g [13], a Néel AFM state for large g , and a twofold degenerate plaquette-singlet (PS) state for $g \in [0.68, 0.77]$ [3,6,14,15].

At ambient pressure $\text{SrCu}_2(\text{BO}_3)_2$ is in the DS phase [1,2] but the other SS phases have been anticipated under high pressure [16]. Recent heat capacity [7,8], neutron scattering [4], and Raman [9] experiments have indeed confirmed some variant [17,18] of the PS phase (from 1.7 to 2.5 GPa at temperatures $T < 2$ K) and an AFM phase (between 3 and 4 GPa below 4 K). A direct PS-AFM transition may then be expected between 2.6 and 3 GPa [19] at temperatures not yet reached.

Here, we show that the above picture is incomplete. Using the density-matrix renormalization group (DMRG) method [20], we study the ground state and low-lying excitations of the SS model. Based on the lattice-size dependence of the level spectrum and order parameters, we conclude that a narrow gapless spin liquid (SL) phase intervenes between the PS and AFM phases. In light of this finding, the absence of

signs of any phase transition between 2.6 and 3 GPa [7,8] opens the intriguing prospect of an SL phase in $\text{SrCu}_2(\text{BO}_3)_2$.

DMRG calculations. The SS model with AFM couplings J between first neighbor spins $\langle ij \rangle$ and J' on a subset of second neighbors $\langle ij' \rangle$ is illustrated in Fig. 1. The Hamiltonian is [13]

$$H = J \sum_{\langle ij \rangle} \mathbf{S}_i \cdot \mathbf{S}_j + J' \sum_{\langle ij' \rangle} \mathbf{S}_i \cdot \mathbf{S}_j, \quad (1)$$

here on $L_x \times L_y$ cylinders [21,22] with open and periodic boundaries in the x and y direction, respectively, and $L \equiv L_y = 2n, L_x = 2L$. In this geometry, the model has a preferred singlet pattern which minimizes the boundary energy in the PS phase; thus the twofold degeneracy is broken and the ground state is unique, as illustrated in Fig. 1.

We have developed efficient procedures for calculating not only the ground state with full $\text{SU}(2)$ symmetry [23,24], but also successively generating excited states by orthogonalizing to previous states [25–27]. Imposing stringent convergence criteria for a given Schmidt number m , we have reached sufficiently large m for reliably extrapolating to discarded weight $\epsilon_m = 0$ (see Supplemental Material [28]) for L up to 10, 12, or 14 depending on quantity (energies and order parameters). Any remaining errors in the results are small on the scale of the graph symbols in the figures presented below.

We focus on the window $g \in [0.7, 0.9]$, which straddles the PS and AFM phases. The ground state of the system is always a singlet, and we analyze the gaps $\Delta(S)$ to the lowest excited singlet ($S = 0$), triplet ($S = 1$), and quintuplet ($S = 2$). Finite-size crossings of excited levels with different spin are often used indicators of quantum phase transitions in spin chains [29–32], and this method was also applied to the 2D J - Q [33] and J_1 - J_2 [26,34,35] Heisenberg models. We here use level

*sandvik@bu.edu

†lingwangqs@zju.edu.cn

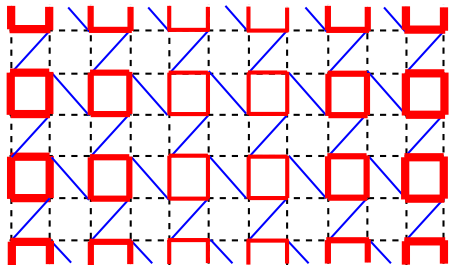


FIG. 1. The SS lattice with open x and periodic y boundary conditions. The lengths L_x and L_y are both even. Nearest neighbors are coupled at strength J by Eq. (1) and the blue diagonal links represent the dimer couplings J' . The open edges break the \mathbb{Z}_2 symmetry of the PS phase, thus inducing a singlet density pattern as indicated schematically by the thickness of the red lines.

crossings to detect the transitions out of the PS phase and into the AFM state, following Ref. [26] closely. We also study the PS and AFM order parameters to corroborate the quantum phases and phase transitions.

We graph singlet and triplet gaps in Fig. 2(a) and similarly singlet and quintuplet gaps in Fig. 2(b), in g windows where gap crossings are observed. In Fig. 3 we analyze the gap crossing points and the singlet minimum that is also observed in Fig. 2(a). Given the previous empirical observations of crossing-point drifts in 2D systems [26,33], we graph the results versus $1/L^2$ and find almost perfect linear behaviors. Interesting, the singlet-triplet crossing and the singlet

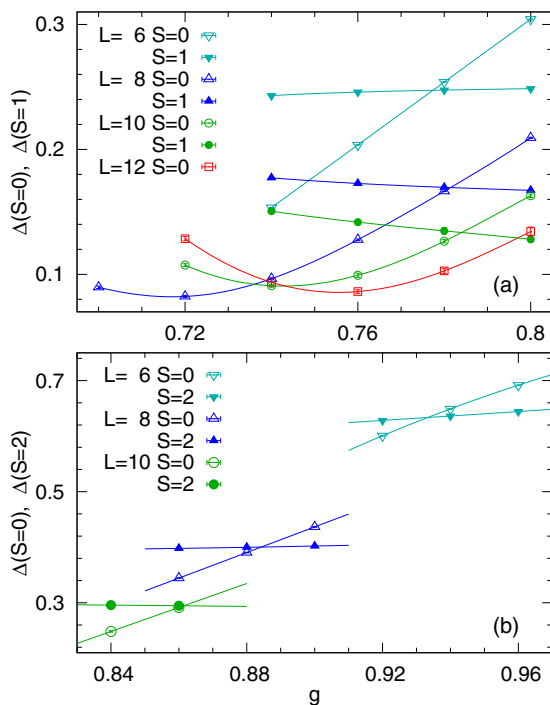


FIG. 2. (a) The lowest singlet and triplet gaps vs g in the neighborhood of the expected quantum phase transition out of the PS phase. (b) The lowest singlet and quintuplet gaps for g inside the AFM phase, close to its quantum phase transition. The curves are polynomial fits.

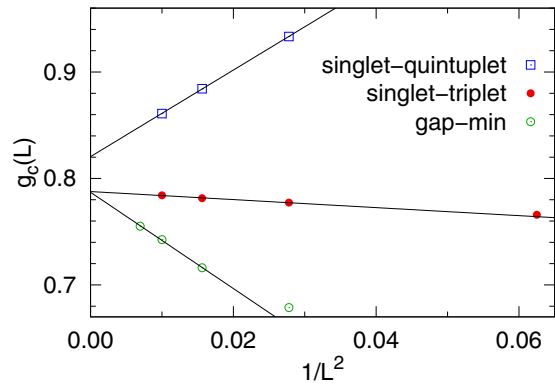


FIG. 3. Locations of gap crossings and singlet minimums, with the lines showing linear-in- $1/L^2$ fits. The $L = 4$ singlet-quintuplet point is at $g \approx 1.1$, falling very close to the fitted line. The extrapolated critical points are $g_{c1} = 0.788 \pm 0.002$ and $g_{c2} = 0.820 \pm 0.002$.

minimum both extrapolate to $g_{c1} \approx 0.79$, while the singlet-quintuplet points scale to a higher value, $g_{c2} \approx 0.82$.

It was previously shown [26,31] that the crossing point between the lowest singlet and quintuplet levels is a useful finite-size estimator for a quantum phase transition into an AFM phase, given that the lowest $S > 0$ states are Anderson quantum rotors, separated from the ground state by gaps $\Delta_A(S) \propto S(S+1)/L^2$, while the singlet excited state should be the gapped amplitude (“Higgs”) mode in the AFM state [6]. In contrast, in other putative phases adjacent to the AFM phase (in the SS model and many other models), the $S = 2$ state will be above the lowest $S = 0$ excitation. Thus, we identify the extrapolated singlet-quintuplet crossing point $g_{c2} \approx 0.82$ with a quantum phase transition into the AFM state.

Following previous work on the J_1 - J_2 model [26], we identify the extrapolated singlet-triplet crossing point $g_{c1} \approx 0.79$ with the transition out of the PS state. The singlet minimum by itself is consistent with the PS gap vanishing at a DQCP and becoming the gapped amplitude mode in the AFM phase [6]. However, an AFM phase starting at g_{c1} is inconsistent with the singlet-quintuplet crossing point g_{c2} . Though the separation between the transition points $g_{c1} \approx 0.79$ and $g_{c2} \approx 0.82$ is small, an eventual flow toward a common point for larger systems appears unlikely, given the absence of significant corrections to the $1/L^2$ forms in Fig. 3. Below we will show evidence for a gapless SL phase for $g \in (g_{c1}, g_{c2})$.

Both gap crossings match those in the J_1 - J_2 Heisenberg model [26], where several numerical studies have reached a consensus on the existence of a gapless SL phase between dimerized and AFM phases [24,26,34–36]. Field theories have also recently been proposed for this SL phase [37,38]. Moreover, the same level crossings were found at the transition from a critical state to either a dimerized state (singlet-triplet crossing) or an AFM state (singlet-quintuplet crossing) in a frustrated Heisenberg chain with long-range interactions [26,31]. Given these results for related models, the distinct g_{c1} and g_{c2} points suggest a gapless SL phase also in the SS model.

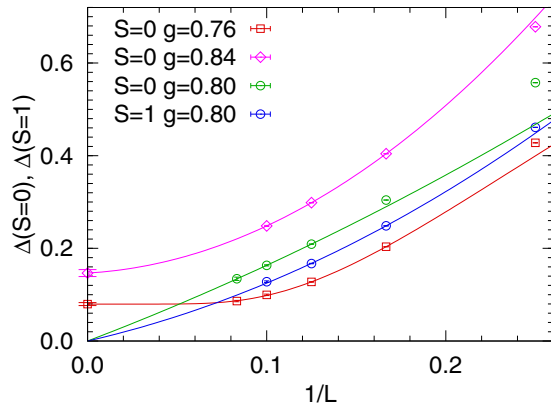


FIG. 4. Gaps vs inverse system size. The singlet and triplet at $g = 0.80$ (SL phase) have been fitted to the form $\Delta = a/L + b/L^2$ (a and b being fitting parameters). The singlets in the PS ($g = 0.76$) and AFM ($g = 0.84$) phases converge to nonzero values, as shown with a fit of the form $\Delta = a + be^{-cL}$ (fitting parameters a, b, c) in the former case and a quadratic form in the latter case.

In Fig. 4 we analyze the size-dependent gaps in and close to the putative SL phase. At $g = 0.80$, both the singlet and triplet gaps exhibit asymptotic $1/L$ scaling, corresponding to a dynamic exponent $z = 1$ inside the SL phase. At $g = 0.76$, in the PS phase, the singlet (and also the not shown triplet) converges exponentially to a nonzero gap, as expected in the SS model with cylindrical boundaries (Fig. 1) for which the shifted PS state is gapped by boundary energies. In the AFM phase, we find convergence to a nonzero amplitude-mode energy at $g = 0.84$. In Fig. 4 we have fitted a polynomial in this case, which works better than an exponentially convergent form, likely due to a gapless spectrum above the lowest singlet (unlike the isolated singlet mode in the PS state).

We next study order parameters. We use the squared AFM magnetization, $m_s^2 = L^{-4} \sum_{ij} \phi_{ij} \langle \mathbf{S}_i \cdot \mathbf{S}_j \rangle$, where i, j are sites in the central $L \times L$ area of a $2L \times L$ system and $\phi_{ij} = \pm 1$ is the staggered phase. To detect PS order we define $\mathbf{Q}_r \equiv \frac{1}{2}(\mathbf{P}_r + \mathbf{P}_r^{-1})$, with \mathbf{P}_r a cyclic permutation operator on the four spins of a plaquette at \mathbf{r} . Given the boundary-induced plaquette pattern (Fig. 1), we can detect the PS order as the difference of $\langle \mathbf{Q}_r \rangle$ on two adjacent “empty” SS plaquettes [39]. Thus, we define $m_p = \langle \mathbf{Q}_R - \mathbf{Q}_{R'} \rangle$, where \mathbf{R} and \mathbf{R}' are both close to the center of the cylinder (the landscape of \mathbf{Q}_r values is shown in the Supplemental Material [28]). Both order parameters are graphed versus $1/L$ in Fig. 5.

Second-order polynomial extrapolations of the AFM order parameter in Fig. 5 show that m_s^2 vanishes for $g \approx 0.82$, thus providing further evidence for the AFM phase starting at the extrapolated singlet-quintuplet point $g_{c2} \approx 0.82$. The polynomial form is strictly appropriate only inside the AFM phase, while at a critical point (or phase) $m_s^2 \propto L^{-(1+\eta)}$ should instead apply asymptotically. The $g = 0.80$ and 0.82 data can indeed be fitted with $\eta \approx 0.32$ and $\eta \approx 0.23$, respectively. In the PS phase, polynomial fits extrapolate to unphysical negative values, which can be understood on account of the expected $\propto L^{-2}$ asymptotic form (which, however, cannot be fitted because of large corrections).

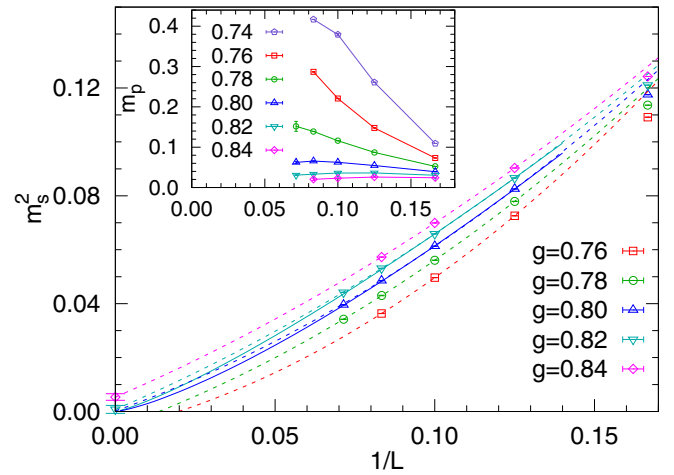


FIG. 5. Squared AFM order parameter vs inverse system size for several g values. The corresponding PS order parameters are shown in the inset. The dashed curves with colors matching the symbols in the main graph are second-order polynomials, while the solid curves are of the critical form $\propto L^{-(1+\eta)}$ with $\eta \approx 0.32$ and $\eta \approx 0.23$ for $g = 0.80$ and 0.82 , respectively. Fitting to the m_p data is not meaningful, but the nonmonotonic behavior for $g = 0.80$ – 0.84 is explained by boundary PS order outside the PS phase (see Supplemental Material [28]) and $m_p \rightarrow 0$ for $L \rightarrow \infty$.

The inset of Fig. 5 shows how PS order is stabilized only for the larger system sizes inside the PS phase, reflecting large fluctuations in small systems (as shown explicitly in the Supplemental Material [28]). The central plaquettes where m_p is defined are close to the cylinder edges for small L , and only for larger L can m_p reflect a disordered bulk. Outside the PS phase the boundary-induced order close to the edges first increases with L , thus causing nonmonotonic behavior as seen most clearly at $g = 0.82$ and 0.84 (see also Supplemental Material [28]). At $g = 0.80$, m_p for $L = 14$ also falls below the value for $L = 12$, indicating that indeed $m_p \rightarrow 0$ when $L \rightarrow \infty$, as it should in the SL phase.

DQCP and unified phase diagram. The originally proposed DQCP is generic, reachable by tuning a single parameter [10]. Quantum Monte Carlo studies of several variants of J - Q Hamiltonians [12] have indeed found direct transitions between AFM and dimerized ground states [40–51]. Similar results have been obtained with related classical loop [52,53] and dimer [54] models. In most cases, no discontinuities were observed, though unusual scaling violations point to weak first-order transitions [41,48,55] or other scenarios [45,50]. One proposal is that the DQCP is unreachable (e.g., existing only in dimensionality below $2 + 1$) and described by a nonunitary conformal field theory (CFT) [56–62].

In some variants of the J - Q model clearly first-order transitions were observed [5,63,64]. The checkerboard J - Q (CBJQ) model [5] (and a closely related loop model [65]) has a \mathbb{Z}_2 breaking PS phase such as that in the SS model. A first-order spin-flop-like transition with emergent $O(4)$ symmetry of the combined $O(3)$ AFM and scalar PS order parameters was found, with no conventional coexistence state with tunneling barriers up to the largest length scales studied. This unusual behavior indicates close proximity to an $O(4)$ DQCP.

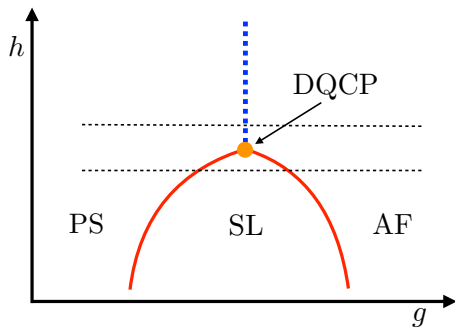


FIG. 6. Unified phase diagram, where an $O(4)$ DQCP separates a line of first-order PS-AFM transitions and an extended SL phase. The PS-SL and SL-AFM transition may both be continuous DQCP-like transitions. The dashed horizontal lines illustrate cuts through the phase diagram when a single parameter g is tuned, corresponding to the CBJQ model (top line) and the SS model (bottom line).

Lee *et al.* recently considered a proxy of the excitation gap with the iDMRG method (infinite-size DMRG, where $L_x \rightarrow \infty$ and L_y is finite), studying correlation lengths of operators with the symmetries of the excited levels of interest [6]. Following Ref. [26], they identified both crossing points discussed here (Figs. 2 and 3), but these points were not extrapolated to infinite size. It was nevertheless argued that the singlet-triplet and singlet-quintuplet crossings will drift to a common DQCP with increasing system size, in the SS model as well as in the J_1 - J_2 model. However, in a very recent work, Shackleton *et al.* revisited the J_1 - J_2 model and constructed a quantum field theory of a gapless SL phase and a DQCP separating it from the AFM state [37]. A different field theory was outlined in Ref. [38].

The narrow SL phase found here in the SS model suggests proximity to the DQCP discussed by Lee *et al.* [6], which most likely would be the same DQCP as the one influencing the $O(4)$ transition in the CBJQ model [5]. Moreover, it has recently been argued that the DQCP is actually a multicritical point [66,67]; a second relevant scaling field with all the symmetries of the Hamiltonian was detected in the conventional critical J - Q model [66], and subsequently such a field was also identified in a deformed self-dual field theory [67]. In the J - Q model it was found that the system flows toward a first-order transition when a certain interaction is turned on in a way maintaining a sign-free path integral [63]. It is possible that the interaction with the opposite sign could instead open up an SL phase. Taken together, all these observations suggest the unified phase diagram schematically illustrated in Fig. 6. The two parameters (g, h) correspond to two relevant symmetric fields, and in models with just one tuning parameter g , e.g., the CBJQ and SS models, either the first-order line or the SL phase is traversed. Possible ways to tune h in a model are further discussed below.

Summary and discussion. Our DMRG results can consistently be explained by a previously not anticipated SL phase between the known PS and AFM phases of the SS model. The PS-SL point $g_{c1} \approx 0.79$ is above the PS-AFM point $g_c \approx 0.765$ obtained with tensor product states [14] (where the system is infinite but the results may be affected by small tensors) but is not at significant variance with the more recent iDMRG

calculation [6], where $g_c \approx 0.77$ for $L = 12$ and an increase in g_c with L was observed (see Table 1 of Ref. [6]). The tensor technique used in Ref. [14] has a bias to ordered phases and may induce AFM order in the fragile SL phase. In Ref. [6] the AFM order parameter was not studied, and its appearance only at higher g may have been missed. While these works did not consider any other phase intervening between the PS and AFM phases, an early field theory of the SS model within an $1/S_i$ expansion (with $S_i = 1/2$ being the target spin value) contains phases not detected numerically to date, including a gapped SL and a helical phase, but no gapless SL [68]. Topological order has also been proposed [69]. As discussed further in the Supplemental Material [28], for all values of g we find the dominant spin correlations at the Néel wave vector $\mathbf{k} = (\pi, \pi)$, i.e., no helical order.

Given our SS results and the existence of a gapless SL in the square-lattice J_1 - J_2 model [24,26,34–37], SLs ending at DQCPs may be ubiquitous between symmetry-breaking singlet and AFM phases. The commonly studied Dirac SLs should be unstable on square lattices and lead to DQCPs [6,70], and the SL identified here should fall outside this framework [37,38]. In our scenario, in a multiparameter model the SL can be shrunk to a multicritical DQCP with emergent symmetry, followed by a first-order direct PS-AFM transition. In principle there could be a triple point instead of the DQCP in Fig. 6, with weak first-order transitions as in the nonunitary CFT proposal [56–60,62].

A DQCP separating a line of first-order transitions and an SL phase is a compelling scenario also considering that the J - Q models can be continuously deformed into conventional frustrated models. Placing Q terms on the empty plaquettes of the SS lattice, by gradually turning off Q and turning on J' the unusual first-order PS-AFM transition with emergent $O(4)$ symmetry of the CBJQ model [5] should evolve as if the upper dashed line in Fig. 6 moved to lower h , and eventually the SS SL phase should appear. In general, we expect that many perturbations of the SS and J_1 - J_2 models could act as the parameter h in Fig. 6, e.g., longer-range interactions or multispin cyclic exchange with appropriate signs. The $O(4)$ symmetry should be replaced by $SO(5)$ in cases where the PS phase is instead a dimerized phase, e.g., with some extensions of the conventional J - Q and J_1 - J_2 models.

An SL phase can explain the absence of any observed phase transition in $\text{SrCu}_2(\text{BO}_3)_2$ at pressures 2.6–3 GPa [7,8], between the PS and AFM phases. Since $\text{SrCu}_2(\text{BO}_3)_2$ can be synthesized with a very low concentration of impurities, unlike many other potential spin liquid materials, an SL phase would be significant. A direct PS-AFM transition has already been observed at high magnetic fields [8], but the nature of the transition remains unexplored. The phase diagram in Fig. 6 may also hold with h corresponding to the field strength, but with the symmetry of the AFM order reduced to $O(2)$ and potentially emergent $O(3)$ symmetry of the DQCP [instead of $O(4)$ at zero field] and on the adjacent direct PS-AFM line.

Note added. A recent functional renormalization group calculation, partially stimulated by our work, supports a gapless SL phase in roughly the same parameter regime as reported here [71]. Moreover, a study with tensor-product states of the J_1 - J_2 - J_3 Heisenberg model detected an isolated SL phase

ending at a DQCP [72], very similar to our phase diagram in Fig. 6 when g and h are identified with J_2/J_1 and J_3/J_1 , respectively (and with a dimerized Z_4 phase instead of the Z_2 PS phase). However, a line of continuous dimerized-AFM transition was proposed beyond the $O(5)$ DQCP, instead of the weakly first-order transitions argued for here.

We would like to thank Frédéric Mila, Zheng-Cheng Gu, Didier Poliblauc, Subir Sachdev, Sriram Shastry, Cenke Xu, and Yi-Zhuang You for stimulating discussions and com-

ments, and Subir Sachdev also for sending us an early version of Ref. [37]. A.W.S. was supported by the Simons Foundation under Simons Investigator Grant No. 511064. L.W. was supported by the National Key Research and Development Program of China, Grant No. 2016YFA0300603, and by the National Natural Science Foundation of China, Grants No. NSFC-11874080 and No. NSFC-11734002. The computational results presented here were achieved partially using Tianhe-2JK computing time awarded by the Beijing Computational Science Research Center (CSRC).

-
- [1] H. Kageyama, K. Yoshimura, R. Stern, N. V. Mushnikov, K. Onizuka, M. Kato, K. Kosuge, C. P. Slichter, T. Goto, and Y. Ueda, Exact Dimer Ground State and Quantized Magnetization Plateaus in the Two-Dimensional Spin System $\text{SrCu}_2(\text{BO}_3)_2$, *Phys. Rev. Lett.* **82**, 3168 (1999).
- [2] S. Miyahara and K. Ueda, Exact Dimer Ground State of the Two Dimensional Heisenberg Spin System $\text{SrCu}_2(\text{BO}_3)_2$, *Phys. Rev. Lett.* **82**, 3701 (1999).
- [3] A. Koga and N. Kawakami, Quantum Phase Transitions in the Shastry-Sutherland Model for $\text{SrCu}_2(\text{BO}_3)_2$, *Phys. Rev. Lett.* **84**, 4461 (2000).
- [4] M. Zayed, Ch. Rüegg, J. Larrea, A. M. Läuchli, C. Panagopoulos, S. S. Saxena, M. Ellerby, D. McMorr, Th. Strässle, S. S. Klotz, G. Hamel, R. A. Sadykov, V. Pomjakushin, M. Boehm, M. Jiménez-Ruiz, A. Schneidewin, E. Pomjakushin, M. Stingaciu, K. Conder, and H. M. Rønnow, 4-spin plaquette singlet state in the Shastry-Sutherland compound $\text{SrCu}_2(\text{BO}_3)_2$, *Nat. Phys.* **13**, 962 (2017).
- [5] B. Zhao, P. Weinberg, and A. W. Sandvik, Symmetry enhanced first-order phase transition in a two-dimensional quantum magnet, *Nat. Phys.* **15**, 678 (2019).
- [6] J. Y. Lee, Y.-Z. You, S. Sachdev, and A. Vishwanath, Signatures of a Deconfined Phase Transition on the Shastry-Sutherland Lattice: Applications to Quantum Critical $\text{SrCu}_2(\text{BO}_3)_2$, *Phys. Rev. X* **9**, 041037 (2019).
- [7] J. Guo, G. Sun, B. Zhao, L. Wang, W. Hong, V. A. Sidorov, N. Ma, Q. Wu, S. Li, Z. Y. Meng, A. W. Sandvik, and L. Sun, Quantum Phases of $\text{SrCu}_2(\text{BO}_3)_2$ from High-Pressure Thermodynamics, *Phys. Rev. Lett.* **124**, 206602 (2020).
- [8] J. Larrea Jiménez, S. P. G. Crone, E. Fogh, M. E. Zayed, R. Lortz, E. Pomjakushina, K. Conder, A. M. Läuchli, L. Weber, S. Wessel, A. Honecker, B. Normand, Ch. Rüegg, P. Corboz, H. M. Rønnow, and F. Mila, A quantum magnetic analogue to the critical point of water, *Nature (London)* **592**, 370 (2021).
- [9] S. Bettler, L. Stoppel, Z. Yan, S. Gvasaliya, and A. Zheludev, Sign switching of dimer correlations in $\text{SrCu}_2(\text{BO}_3)_2$ under hydrostatic pressure, *Phys. Rev. Research* **2**, 012010(R) (2020).
- [10] T. Senthil, A. Vishwanath, L. Balents, S. Sachdev, and M. P. A. Fisher, Deconfined quantum critical points, *Science* **303**, 1490 (2004).
- [11] S. Sachdev, Quantum magnetism and criticality, *Nat. Phys.* **4**, 173 (2008).
- [12] A. W. Sandvik, Evidence for Deconfined Quantum Criticality in a Two-Dimensional Heisenberg Model with Four-Spin Interactions, *Phys. Rev. Lett.* **98**, 227202 (2007).
- [13] B. S. Shastry and B. Sutherland, Exact ground state of a quantum mechanical antiferromagnet, *Physica B+C* **108**, 1069 (1981).
- [14] P. Corboz and F. Mila, Tensor network study of the Shastry-Sutherland model in zero magnetic field, *Phys. Rev. B* **87**, 115144 (2013).
- [15] H. Nakano and T. Sakai, Third boundary of the Shastry-Sutherland model by numerical diagonalization, *J. Phys. Soc. Jpn.* **87**, 123702 (2018).
- [16] T. Waki, K. Arai, M. Takigawa, Y. Saiga, Y. Uwatoko, H. Kageyama, and Y. Ueda, A novel ordered phase in $\text{SrCu}_2(\text{BO}_3)_2$ under high pressure, *J. Phys. Soc. Jpn.* **76**, 073710 (2007).
- [17] C. Boos, S. P. G. Crone, I. A. Niesen, P. Corboz, K. P. Schmidt, and F. Mila, Competition between intermediate plaquette phases in $\text{SrCu}_2(\text{BO}_3)_2$ under pressure, *Phys. Rev. B* **100**, 140413(R) (2019).
- [18] Z. Shi, S. Dissanayake, P. Corboz, W. Steinhardt, D. Graf, D. M. Silevitch, H. A. Dabkowska, T. F. Rosenbaum, F. Mila, and S. Haravifard, Phase diagram of the Shastry-Sutherland Compound $\text{SrCu}_2(\text{BO}_3)_2$ under extreme combined conditions of field and pressure, [arXiv:2107.02929](https://arxiv.org/abs/2107.02929).
- [19] G. Sun, N. Ma, B. Zhao, A. W. Sandvik, and Z. Y. Meng, Emergent $O(4)$ symmetry at the phase transition from plaquette-singlet to antiferromagnetic order in quasi-two-dimensional quantum magnets, *Chin. Phys. B* **30**, 067505 (2021).
- [20] S. R. White, Density Matrix Formulation for Quantum Renormalization Groups, *Phys. Rev. Lett.* **69**, 2863 (1992).
- [21] U. Schollwöck, The density-matrix renormalization group in the age of matrix product states, *Ann. Phys. (Amsterdam)* **326**, 96 (2011).
- [22] E. M. Stoudenmire and S. R. White, Real-space parallel density matrix renormalization group, *Phys. Rev. B* **87**, 155137 (2013).
- [23] A. Weichselbaum, Non-Abelian symmetries in tensor networks: A quantum symmetry space approach, *Ann. Phys. (Amsterdam)* **327**, 2972 (2012).
- [24] S.-S. Gong, W. Zhu, D. N. Sheng, O. I. Motrunich, and M. P. A. Fisher, Plaquette Ordered Phase and Quantum Phase Diagram in the Spin-1/2 J_1 - J_2 Square Heisenberg Model, *Phys. Rev. Lett.* **113**, 027201 (2014).
- [25] I. P. McCulloch, From density-matrix renormalization group to matrix product states, *J. Stat. Mech.* (2007) P10014.
- [26] L. Wang and A. W. Sandvik, Critical Level Crossings and Gapless Spin Liquid in the Square-Lattice Spin-1/2 J_1 - J_2 Heisenberg Antiferromagnet, *Phys. Rev. Lett.* **121**, 107202 (2018).

- [27] M. Lemm, A. W. Sandvik, and L. Wang, Existence of a Spectral Gap in the Affleck-Kennedy-Lieb-Tasaki Model on the Hexagonal Lattice, *Phys. Rev. Lett.* **124**, 177204 (2020).
- [28] See Supplemental Material at <http://link.aps.org/supplemental/10.1103/PhysRevB.105.L060409> for DMRG convergence procedures and extrapolations, the 2D real-space landscape of PS ordering, and the spin structure factor.
- [29] K. Nomura and K. Okamoto, Fluid-dimer critical point in $S = 1/2$ antiferromagnetic Heisenberg chain with next nearest neighbor interactions, *Phys. Lett. A* **169**, 433 (1992).
- [30] S. Eggert, Numerical evidence for multiplicative logarithmic corrections from marginal operators, *Phys. Rev. B* **54**, R9612 (1996).
- [31] A. W. Sandvik, Ground States of a Frustrated Quantum Spin Chain with Long-Range Interactions, *Phys. Rev. Lett.* **104**, 137204 (2010).
- [32] H. Suwa and S. Todo, Generalized Moment Method for Gap Estimation and Quantum Monte Carlo Level Spectroscopy, *Phys. Rev. Lett.* **115**, 080601 (2015).
- [33] H. Suwa, A. Sen, and A. W. Sandvik, Level spectroscopy in a two-dimensional quantum magnet: Linearly dispersing spinons at the deconfined quantum critical point, *Phys. Rev. B* **94**, 144416 (2016).
- [34] Y. Nomura and M. Imada, Dirac-Type Nodal Spin Liquid Revealed by Machine Learning, *Phys. Rev. X* **11**, 031034 (2021).
- [35] F. Ferrari and F. Becca, Gapless spin liquid and valence-bond solid in the J_1 - J_2 Heisenberg model on the square lattice: Insights from singlet and triplet excitations, *Phys. Rev. B* **102**, 014417 (2020).
- [36] S. Morita, R. Kaneko, and M. Imada, Quantum spin liquid in spin $1/2J_1$ - J_2 Heisenberg model on square lattice: Many-variable variational Monte Carlo study combined with quantum-number projections, *J. Phys. Soc. Jpn.* **84**, 024720 (2015).
- [37] H. Shackleton, A. Thomson, and S. Sachdev, Deconfined criticality and a gapless \mathbb{Z}_2 spin liquid in the square lattice antiferromagnet, *Phys. Rev. B* **104**, 045110 (2021).
- [38] W.-Y. Liu, S.-S. Gong, Y.-B. Li, D. Poilblanc, W.-Q. Chen, and Z.-C. Gu, Gapless quantum spin liquid and global phase diagram of the spin- $1/2$ J_1 - J_2 square antiferromagnetic Heisenberg model, [arXiv:2009.01821](https://arxiv.org/abs/2009.01821).
- [39] B. Zhao, J. Takahashi, and A. W. Sandvik, Comment on “Gapless spin liquid ground state of the spin-1 J_1 - J_2 Heisenberg model on square lattices”, *Phys. Rev. B* **101**, 157101 (2020).
- [40] R. G. Melko and R. K. Kaul, Scaling in the Fan of an Unconventional Quantum Critical Point, *Phys. Rev. Lett.* **100**, 017203 (2008).
- [41] F.-J. Jiang, M. Nyfeler, S. Chandrasekharan, and U.-J. Wiese, From an antiferromagnet to a valence bond solid: evidence for a first-order phase transition, *J. Stat. Mech.: Theory Exp.* (2008) P02009.
- [42] J. Lou, A. W. Sandvik, and N. Kawashima, Antiferromagnetic to valence-bond-solid transitions in two-dimensional $SU(N)$ Heisenberg models with multispin interactions, *Phys. Rev. B* **80**, 180414(R) (2009).
- [43] A. W. Sandvik, Continuous Quantum Phase Transition between an Antiferromagnet and a Valence-Bond Solid in Two Dimensions: Evidence for Logarithmic Corrections to Scaling, *Phys. Rev. Lett.* **104**, 177201 (2010).
- [44] R. K. Kaul, Quantum criticality in $SU(3)$ and $SU(4)$ antiferromagnets, *Phys. Rev. B* **84**, 054407 (2011).
- [45] A. W. Sandvik, Finite-size scaling and boundary effects in two-dimensional valence-bond solids, *Phys. Rev. B* **85**, 134407 (2012).
- [46] M. S. Block, R. G. Melko, and R. K. Kaul, Fate of $\mathbb{C}\mathbb{P}^{N-1}$ Fixed Points with q Monopoles, *Phys. Rev. Lett.* **111**, 137202 (2013).
- [47] K. Harada, T. Suzuki, T. Okubo, H. Matsuo, J. Lou, H. Watanabe, S. Todo, and N. Kawashima, Possibility of deconfined criticality in $SU(N)$ Heisenberg models at small N , *Phys. Rev. B* **88**, 220408(R) (2013).
- [48] K. Chen, Y. Huang, Y. Deng, A. B. Kuklov, N. V. Prokof'ev, and B. V. Svistunov, Deconfined Criticality Flow in the Heisenberg Model with Ring-Exchange Interactions, *Phys. Rev. Lett.* **110**, 185701 (2013).
- [49] S. Pujari, F. Alet, and K. Damle, Transitions to valence-bond solid order in a honeycomb lattice antiferromagnet, *Phys. Rev. B* **91**, 104411 (2015).
- [50] H. Shao, W. Guo, A. W. Sandvik, Quantum criticality with two length scales, *Science* **352**, 213 (2016).
- [51] A. W. Sandvik and B. Zhao, Consistent scaling exponents at the deconfined quantum-critical point, *Chin. Phys. Lett.* **37**, 057502 (2020).
- [52] A. Nahum, P. Serna, J. T. Chalker, M. Ortuño, and A. M. Somoza, Emergent $SO(5)$ Symmetry at the Néel to Valence-Bond-Solid Transition, *Phys. Rev. Lett.* **115**, 267203 (2015).
- [53] A. Nahum, J. T. Chalker, P. Serna, M. Ortuño, and A. M. Somoza, Deconfined Quantum Criticality, Scaling Violations, and Classical Loop Models, *Phys. Rev. X* **5**, 041048 (2015).
- [54] G. J. Sreejith, S. Powell, and A. Nahum, Emergent $SO(5)$ Symmetry at the Columnar Ordering Transition in the Classical Cubic Dimer Model, *Phys. Rev. Lett.* **122**, 080601 (2019).
- [55] Z. Wang, M. P. Zaletel, R. S. K. Mong, and F. F. Assaad, Phases of the (2+1) Dimensional $SO(5)$ Nonlinear Sigma Model with Topological Term, *Phys. Rev. Lett.* **126**, 045701 (2021).
- [56] C. Wang, A. Nahum, M. A. Metlitski, C. Xu, and T. Senthil, Deconfined Quantum Critical Points: Symmetries and Dualities, *Phys. Rev. X* **7**, 031051 (2017).
- [57] V. Gorbenco, S. Rychkov, and B. Zan, Walking, weak first-order transitions, and complex CFTs, *J. High Energy Phys.* **10** (2018) 108.
- [58] V. Gorbenco, S. Rychkov, and B. Zan, Walking, Weak first-order transitions, and Complex CFTs II. Two-dimensional Potts model at $Q > 4$, *SciPost Phys.* **5**, 050 (2018).
- [59] R. Ma and C. Wang, A theory of deconfined pseudocriticality, *Phys. Rev. B* **102**, 020407(R) (2020).
- [60] A. Nahum, Note on Wess-Zumino-Witten models and quasi-universality in 2+1 dimensions, *Phys. Rev. B* **102**, 201116(R) (2020).
- [61] Z. Li, Solving QED_3 with conformal bootstrap, [arXiv:1812.09281](https://arxiv.org/abs/1812.09281).
- [62] Y.-C. He, J. Rong, and N. Su, Non-Wilson-Fisher kinks of $O(N)$ numerical bootstrap: from the deconfined phase transition to a putative new family of CFTs, *SciPost Phys.* **10**, 115 (2021).
- [63] B. Zhao, J. Takahashi, and A. W. Sandvik, Tunable deconfined quantum criticality and interplay of different valence-bond solid phases, *Chin. Phys. B* **29**, 057506 (2020).
- [64] J. Takahashi and A. W. Sandvik, Valence-bond solids, vestigial order, and emergent $SO(5)$ symmetry in a two-

- dimensional quantum magnet, [Phys. Rev. Research **2**, 033459 \(2020\)](#).
- [65] P. Serna and A. Nahum, Emergence and spontaneous breaking of approximate $O(4)$ symmetry at a weakly first-order deconfined phase transition, [Phys. Rev. B **99**, 195110 \(2019\)](#)
- [66] B. Zhao, J. Takahashi, and A. W. Sandvik, Multicritical Deconfined Quantum Criticality and Lifshitz Point of a Helical Valence-Bond Phase, [Phys. Rev. Lett. **125**, 257204 \(2020\)](#).
- [67] D.-C. Lu, C. Xu, and Y.-Z. You, Self-duality protected multicriticality in deconfined quantum phase transitions, [Phys. Rev. B **104**, 205142 \(2021\)](#).
- [68] C. H. Chung, J. B. Marston, and S. Sachdev, Quantum phases of the Shastry-Sutherland antiferromagnet: Application to $\text{SrCu}_2(\text{BO}_3)_2$, [Phys. Rev. B **64**, 134407 \(2001\)](#).
- [69] D. C. Ronquillo and M. R. Peterson, Identifying topological order in the Shastry-Sutherland model via entanglement entropy, [Phys. Rev. B **90**, 201108\(R\) \(2014\)](#).
- [70] X.-Y. Song, Y.-C. He, A. Vishwanath, and C. Wang, From Spinon Band Topology to the Symmetry Quantum Numbers of Monopoles in Dirac Spin Liquids, [Phys. Rev. X **10**, 011033 \(2020\)](#).
- [71] A. Keles and E. Zhao, Rise and fall of plaquette order in the Shastry-Sutherland magnet revealed by pseudofermion functional renormalization group, [Phys. Rev. B **105**, L041115 \(2022\)](#).
- [72] W.-Y. Liu, J. Hasik, S.-S. Gong, D. Poilblanc, W.-Q. Chen, and Z.-C. Gu, The emergence of gapless quantum spin liquid from deconfined quantum critical point, [arXiv:2110.11138](#).